Cancer Chemother Pharmacol (2005) 56: 497–509
DOI 10.1007/s00280-005-1001-8

ORIGINAL ARTICLE

Ramin Darvari · Mehdi Boroujerdi

Investigation of the influence of modulation of *P*-glycoprotein by a multiple dosing regimen of tamoxifen on the pharmacokinetics and toxicodynamics of doxorubicin

Received: 5 October 2004 / Accepted: 7 February 2005 / Published online: 4 June 2005

Abstract *Purpose*: The in vivo effect of modulators of *P*-glycoprotein (Pgp) on organ accumulation of substrates of Pgp has not been fully investigated. We investigated the influence of a Pgp modulator (tamoxifen, TAM) on the pharmacokinetics and toxicodynamics of a Pgp substrate (doxorubicin, DOX) in rats. *Methods*: TAM was administered daily for 11 days before the administration of DOX in male Sprague-Dawley rats, with all doses being clinically relevant. The experimental design of the project consisted of two different protocols. One was to investigate the effect of DOX on the time course of Pgp-ATPase activity, sarcoplasmic reticulum Ca^{2+}-ATPase (SERCA) activity, and DOX concentration in the heart, liver, and kidneys of TAM-pretreated animals; the other protocol was to study the effect of TAM pretreatment on the disposition of DOX in the body by investigating its time course in plasma, urine and bile. *Results*: The simultaneous curve fitting of plasma data with urine and bile data with the help of the related pharmacokinetic equations provided the calculated parameters and constants. The first-order rate constants between the central and the myocardial compartments (k_{1H} and k_{H1}) were decreased in the TAM-treated group. The treatment also significantly reduced the k_{1H}/k_{H1} ratio in comparison to that of the control group. The first-order biliary elimination rate constant (k_b) was significantly decreased (29%) in the TAM-treated group. The reduction was estimated in comparison with that of the control group. This reduction could be attributed to the inhibitory effect of TAM on Pgp located on biliary canicular membranes. The initial reduction of Pgp activity in TAM-treated group was at 60% of the basal level. The activity declined and reached a plateau at 20% of the basal activity after 6 h and remained at that level for 24 h. The area under the curves of Pgp-ATPase activity time ($AUC_{Activity\ 0\text{-}24}$) following DOX administration in TAM-treated group was significantly lower than that of the control group, indicating an overall inhibitory effect of TAM on Pgp-ATPase activity under the protocol of this study. The area under the curves of the SERCA activity-time curve following DOX administration in TAM-treated group demonstrated a 15% reduction in $AUC_{Activity\ 0\text{-}24}$ in comparison with that of the control group, an indication of increased toxicity. The amount of myocardial Pgp in the 24-h period following DOX administration was comparable to the control group and showed no significant deviation from the basal levels of the protein. *Conclusions*: The effect of TAM on DOX accumulation in the myocardial tissue and the increase in cardiotoxicity can be related to the net inhibitory effect of TAM on the efflux activity of Pgp in the heart. The results of the present study supported the hypothesis of the project that multiple regimen pretreatment with Pgp modulator TAM increases the DOX accumulation in the heart and promotes DOX-induced cardiotoxicity.

Glycoprotein · Tamoxifen · Pharmacokinetics · Doxorubicin

R. Darvari
Epic Therapeutics Inc., a Subsidiary of Baxter Healthcare Corporation, 220 Norwood Park South, Norwood, MA 02062, USA

Present address: M. Boroujerdi (✉)
Massachusetts College of Pharmacy and Health Sciences, Department of Pharmaceutical Sciences, Pharmacokinetics and Drug Metabolism Laboratory, 179 Longwood Ave, Boston, MA 02115, USA
E-mail: mehdi.boroujerdi@bos.mcphs.edu
Tel.: +(617) 732 2108
Fax: +(617) 735 1082

Introduction

P-glycoprotein (Pgp) plays a major role in the cellular efflux of a number of structurally diverse xenobiotics. Hydrophobicity and amphipathicity have been suggested as the common characteristics of these molecules [1, 2]. The rate and magnitude of the efflux are directly proportional to the magnitude of Pgp. The tissues with

highly expressed Pgp influence the disposition and uptake of drugs and thus their therapeutic effectiveness or toxic outcome. Examples of tissues with highly expressed Pgp are: tumor cells, the adrenal cortical cells, the brush border of the renal proximal tubule epithelium, the lumenal surface of biliary hepatocytes, small and large intestine mucosal cells, and pancreatic ductules [3–5]. Also, the capillary endothelial cells of the brain, testes, heart, placenta, lungs, prostate, and stomach have been shown to express Pgp at lower levels [4, 6]. Pgp-associated multiple-drug resistance (MDR) in tumor cells and its reversal have been the main focus of many studies. There are, however, parallel physiological consequences related to the presence, activity, and modulation of Pgp in normal cells and tissues. For instance, Pgp plays an important role in renal excretion of its substrates, and administration of inhibitors of Pgp can significantly modify renal excretion and therefore the disposition profile of the substrates [7, 9]. Also, the modulation of Pgp modifies the biliary excretion of the substrates, a phenomenon known as Phase III detoxification [10, 11]. Thus, co-administration of a substrate of Pgp with an inhibitor or a modulator of Pgp may modify the expected pharmacokinetics, pharmacodynamics, and therapeutic/toxic outcome of the substrate [12–15].

Among the substrates of Pgp there are several members of anthracycline anticancer drugs, such as doxorubicin (DOX), epirubicin, and daunorubicin [16–19]. In vitro and in vivo studies have shown that co-administration of DOX and modulators of Pgp such as cyclosporin A, verapamil, PSC 833, and amiodarone results in an increase in cardiotoxicity [20–22]. The study with verapamil showed a significant increase in the area under the curve of myocardial DOX concentration versus time in verapamil-treated animals. Another example of such interaction is the effect of tamoxifen (TAM) on the pharmacokinetics and cardiotoxicity of DOX [23]. In vitro transport studies have shown that TAM has an inhibitory effect on Pgp efflux activity [24, 25]. However, the study on reconstituted liposome-integrated Pgp showed that the inhibition is concentration-dependent and biphasic [26]. Other studies have shown that TAM acts as a modulator of Pgp in a concentration-dependent manner [12]. Thus, its influence as an inhibitor or a stimulator of Pgp in vivo would depend on the overall administered dose, total accumulation of TAM in the body, and concentration of TAM at the Pgp environment.

Measuring the Pgp-ATPase activity is an approach for determining the inhibition or stimulation of Pgp. The activity of Pgp-ATPase to some extent depends on the composition and characteristics of the lipid environment surrounding this enzyme. TAM is known to modify the characteristics of the lipid bilayer. The modification is mainly related to reduction of membrane fluidity, stimulation of phosphatidylethanolamine hydrolysis [27], inhibition of phosphatidyl-ethanolamine synthesis, and inhibition of ethanolamine phosphorylation [28].

The effect of TAM as a Pgp-modulator in cardiotoxicity of DOX remains unclear. The complexity of the interaction stems from multiple properties of TAM. In addition to being a Pgp modulator, TAM has antioxidant property, is a membrane fluidity modifier, and reverses the reduction of levels of certain cardiac detoxifying enzymes such as glutathione peroxidase and glutathione reductase by DOX [29].

We investigated the influence of modulation of Pgp by a multiple-dosing regimen of TAM on the pharmacokinetics and toxicodynamics of doxorubicin in rats. We postulated that although an inhibitor of Pgp reverses the Pgp-dependent multi-drug resistance and improves the potency of chemotherapeutic agents, it can also influence the cellular accumulation of these agents by normal tissues of Pgp-expressing organs and may cause organ toxicity.

Materials and methods

Compounds and reagents

Doxorubicin and epirubicin (as HCl salt) were provided by Pharmacia Upjohn (Albuquerque, NM, USA). Tamoxifen (citrate salt) and daunorubicin were purchased from Sigma Chemical (St. Louis, MO, USA). All other reagents were of analytical or HPLC grade

Animals

Male Sprague-Dawley rats (250–330 g) were used as the animal models. The animals were kept under a 12-h dark/light cycle in a clean environment and had access to standard food and water ad libitum. They were weighed daily at approximately the same time, and the dosage of drugs administered was adjusted accordingly. The protocols for the experiment were approved by the Northeastern University Institutional Animal Care and Use Committee, and all animals were used as per the rules and guidelines of the American Association for Accreditation of Laboratory Animal care (AALAC).

Experimental design

Protocol 1

This experiment was designed to investigate the effect of DOX on the time course of Pgp-ATPase activity, sarcoplasmic reticulum (SR) Ca^{2+} -ATPase activity, and concentrations of DOX in the heart, liver, and kidney of TAM-treated animals. Corn oil was used as the vehicle to prepare the oral dose of TAM. A total of 57 rats were randomly divided into four groups, designated as control 1 ($n=4$), control 2 ($n=27$) and TAM ($n=26$). The TAM-pretreated group was given a daily dose of TAM (1 mg/kg) for 11 consecutive days, followed by a single

intravenous dose of DOX (10 mg/kg, via the tail vein) 1 h after administration of the last dose of TAM. From the TAM-treated group 20 rats were further divided into five subgroups ($n=4$/subgroup). Animals in each subgroup were killed by decapitation at 1, 3, 6, 12, and 24 h after DOX administration.

The rats in control 1 and control 2 groups received daily single doses of corn oil for 11 consecutive days. The animals in control 1 were injected normal saline through the tail vein 1 h after the last dose of corn oil and killed within 1 h after the injection. A total of 20 rats from control 2 received a single 10 mg/kg tail vein injection of DOX 1 h after the last oral dose of corn oil. Twenty animals in control 2 were further divided into five subgroups ($n=4$/subgroup). Animals in each subgroup were killed 1, 3, 6, 12, and 24 h after DOX administration and blood, heart, liver, and kidneys were collected. Blood samples were collected in heparinized glass beakers, centrifuged and the plasma was removed and stored at −20°C until analysis. The urine samples were collected periodically from the 24 h subgroups after receiving DOX. The collected samples were centrifuged and the supernatants stored at −20°C until analysis.

Protocol 2

This protocol was used to study the pharmacokinetics of DOX based on simultaneous sampling of blood and bile following pretreatment with TAM. After the last dose of TAM, the remaining rats from control 2 ($n=7$) and the TAM-treated group ($n=6$) were catheterized through the bile duct and tail vein during sodium pentobarbital anesthesia. A bolus dose of DOX (10 mg/kg) was injected through the tail catheter 1 h after the last oral dose of the TAM and corn oil. Blood (150–200 μl), and bile samples (0.2–2 ml) were collected 5, 15, 30, 45 min and 1, 2, 3, 4, 5, and 6 h after DOX administration. Blood samples were treated as described previously. Bile samples were flash-frozen and stored at −20°C until analysis. Anesthesia was maintained over the course of the experiment.

Homogenization and preparation of subcellular fractions

The heart was homogenized in ice-cold homogenization buffer (20 mM HEPES, 0.3 M KCl, and 0.3 M sucrose, pH 8.4) and was diluted to a final concentration of 100 mg wet weight/ml. The liver and kidney homogenates were prepared by homogenizing approximately 1 g of the median lobe of each liver or whole right kidney in 0.1 M HEPES, pH 7.5. The homogenates were diluted to a final concentration of 200 mg wet weight/ml.

The subcellular fractions of the heart homogenates were prepared at 4°C using differential centrifugation of 9,000 *g* for 20 min, followed by centrifugation of the supernatant (S1) at 100,000 *g* for 30 min. The resultant supernatant (S2) was removed, frozen in liquid nitrogen, and stored at −20°C. The pellet (P2) was then reconstituted in the same buffer, frozen in liquid nitrogen, and stored at −20°C. The protein content of P2 and S2 was determined by the Biuret method with BSA as standard.

Sample preparation for determination of DOX concentration in the tissue homogenates and plasma was conducted according to the method of Anderson et al. [30].

Measurement of ATPase activities

Sarcoplasmic reticulum Ca^{2+} -ATPase (SERCA) activity was measured in the heart homogenates using the method of Simonides et al. [31]. The inorganic phosphate was measured to determine the activity. The difference between the total activity in the presence and absence of 80 nM thapsigargin, a specific inhibitor of SERCA [17], was used as an indicator of the enzyme activity. A modified colorimetric method of Saheki et al. [32] was used to detect inorganic phosphate liberation in the assay medium. The assay medium lacking the homogenate was used as the blank solution.

Pgp-ATPase activity was measured in P2 subcellular fractions of the hearts. Specific inhibition of Pgp ATPase activity was achieved by incubation of the fraction with C219 antibody. C219 is a monoclonal antibody that interacts with ATPase domains of Pgp and prevents their activity [33]. The assay medium (200 μl) contained buffer B (10 mM Tris buffer, pH 8.0, 2 mM $MgCl_2$, 100 mM NaCl, 10 mM KCl, 1 mM dithioerythritol (DTE), and 10 mM 2,3-butanedione monoxime), 4 mM Na-ATP, and 100 mg/ml of P2 subcellular fraction. The assay medium was incubated at 37°C for 30 min with or without C219 (Dako, Carpinteria, CA, USA) prior to addition of the substrate.

Western blot analysis

SDS-PAGE was carried out to separate 10 μg of the P2-fraction proteins on 7.5% polyacrylamide gels, using a Penguin (Owl Seperation Systems, Portsmouth, NH, USA) vertical electrophoresis apparatus. The separated bands on each gel were transferred onto a polyvinylidene fluoride (PVDF) sheet (Costar, Cambridge, MA, USA) using a Panther electroblotting apparatus (Owl Seperation Systems, Portsmouth, NH, USA). Unspecific blocking was achieved by using 5% nonfat dried milk (Carnation/Nestle, Solon, OH, USA) in PBS-T (10 mM phosphate, 0.15 M NaCl, 0.1% Tween-20, pH 7.4) for 1 h at room temperature. After several washings with PBS-T, the sheet was incubated with a 0.2 g/ml solution of the Pgp-specific antibody C219 (Signet, Dedham, MA, USA) in the same buffer at room temperature [34]. The blots were detected using the enhanced chemiluminescence kit from Amersham (Piscataway, NJ, USA). Quantification of Pgp bands was performed using Scion

Image (Scion, Frederick, MD, USA) densitometer software.

HPLC analysis

Separation of DOX and its metabolites was carried out on Nova Pak C-18 cartridge column (3.9 mm×50 mm, particle size 4 μm) in conjunction with a Radial Compression Module and a C-18 Nova pak guard column (Waters, Milford, MA, USA). The mobile phase contained a 0.28 M sodium formate buffer (pH 3.51 at room temperature), acetone, and isopropanol (72.5:25:2.5, respectively) [30]. The final pH of the solution was 4.0 at room temperature. The fluorometric detection of DOX was achieved at excitation and emission wavelengths of 480 nm and 540 nm, respectively. Chromatographic peak and resolution of DOX were verified and quantified by means of retention time and standard curves of the authentic standard. Epirubicin or daunorubicin was used as the internal standards.

Data analysis

An *F*-test was used to examine the equality of unknown variances for the independent random samples. A two-tailed unpaired *t*-test was used to determine statistical differences between the sample means with respect to equality of the variances. Microsoft Exel 97 SR-2 (Microsoft Corp., Redmond, WA, USA) was used to perform the statistical calculations. Pharmacokinetic model fitting was based on the assumptions that the data followed a normal (Gaussian) distribution and that the parameters were independent. The statistical criteria used to study the goodness of fit based on maximum likelihood were Akaike's information criteria (AIC), Schwartz criteria (SC), and the sum of the squares of the errors [35]. WinNonlin software Versions 3.0 (Pharsight Corp., Mountain View, CA, USA) was used in model selection and fitting.

Pharmacokinetic models

Thorough examination of the data based on the selection criteria supported the use of a two-compartment model (model I) for the TAM-treated group and a three-compartment model (model II) for the control group [36].

The following equations describe the rate of change of DOX amount in the central and peripheral compartments (Eqs. 1 and 2), and the related integrated equation (Eq. 3) in TAM-treated animals:

$$V_1 \frac{\mathrm{d}C\mathrm{p}}{\mathrm{d}t} = \frac{\mathrm{d}A_1}{\mathrm{d}t} = k_{21}A_2 - k_{12}A_1 - k_{10}A_1 \tag{1}$$

$$\frac{\mathrm{d}A_2}{\mathrm{d}t} = k_{12}A_1 - k_{21}A_2 \tag{2}$$

$$C\mathrm{p} = A\mathrm{e}^{-\alpha t} + B\mathrm{e}^{-\beta t} \tag{3}$$

where A_1 is the amount of drug in the central compartment at time t; C_p is plasma concentration at time t; V_1 is apparent volume of distribution of the central compartment; A_2 is the amount of drug in the peripheral compartment at anytime t; k_{12} and k_{21} are first-order distribution rate constants from the central to the peripheral compartment, and from the peripheral to the central compartment, respectively; k_{10} is the overall rate constant for elimination of the drug through metabolism and excretion from the system; α and β are the hybrid first-order rate constants of disposition; and A and B are the Y-intercepts of the residual line and the terminal portion of the curve, respectively. The elimination of DOX from the body is defined by the sum of three elimination processes, namely, biliary excretion of DOX (k_b), urinary excretion of DOX (k_e), and elimination through metabolism (k_m), i.e.,

$$k_{10} = k_\mathrm{b} + k_\mathrm{e} + k_\mathrm{m} \tag{4}$$

where, k_{10} is the overall first-order elimination rate constant [6].

With the aid of model-selection criteria, three-compartment model was identified as the appropriate model for analysis of data from the control group. The related differential equations of the model describing the rate of change of DOX in the central (Eq. 5), second (Eq. 6) and third (Eq. 7) compartments and the integrated equation (Eq. 8) are:

$$V_1 \frac{\mathrm{d}C\mathrm{p}}{\mathrm{d}t} = \frac{\mathrm{d}A_1}{\mathrm{d}t} = k_{21}A_2 + k_{31}A_3 - k_{12}A_1 - k_{13}A_1 - k_{10}A_1 \tag{5}$$

$$\frac{\mathrm{d}A_2}{\mathrm{d}t} = k_{12}A_1 - k_{21}A_2 \tag{6}$$

$$\frac{\mathrm{d}A_3}{\mathrm{d}t} = k_{13}A_1 - k_{31}A_3 \tag{7}$$

$$C\mathrm{p} = A\mathrm{e}^{-\alpha t} + B\mathrm{e}^{-\beta t} + C\mathrm{e}^{-\gamma t} \tag{8}$$

where, A_2 and A_3 are the amount of DOX in the second compartment and third compartment at time t, respectively; k_{12}, k_{21}, k_{13} and k_{31} are first-order distribution rate constants between the central and the peripheral compartments; α, β and γ are hybrid first-order rate constants of disposition; A, B and C are Y-intercepts of corresponding exponential terms [36].

The following differential equations describe the rate of biliary or urinary excretion of DOX in the TAM-treated (Eq. 9) and control groups (Eq. 10).

$$\frac{\mathrm{d}A_\mathrm{E}}{dt} = k_\mathrm{E}A_1 = k_\mathrm{E}\left(A\mathrm{e}^{-\alpha t} + B\mathrm{e}^{-\beta t}\right) \tag{9}$$

$$\frac{dA_E}{dt} = k_E A_1 = k_E\left(Ae^{-\alpha t} + Be^{-\beta t} + Ce^{\gamma t}\right) \quad (10)$$

where, A_E is the cumulative amount of DOX excreted in the bile (A_b) or urine (A_e) at time t, k_E is the first-order rate constant of biliary (k_b) or urinary (k_e) excretion of DOX from the central compartment.

The integrated equations to describe the relationship between the cumulative amounts of DOX excreted in the bile or urine of TAM-treated (Eq. 11) and control (Eq. 12) groups with respect to time are:

$$A_E = k_E\left(\frac{A}{\alpha} + \frac{B}{\beta}\right) - k_E\left(\frac{Ae^{-\alpha t}}{\alpha} + \frac{Be^{-\beta t}}{\beta}\right) \quad (11)$$

$$A_E = k_E\left(\frac{A}{\alpha} + \frac{B}{\beta} + \frac{C}{\gamma}\right) - k_E\left(\frac{Ae^{-\alpha t}}{\alpha} + \frac{Be^{-\beta t}}{\beta} + \frac{Ce^{-\gamma t}}{\gamma}\right) \quad (12)$$

Accordingly, the total amount of DOX excreted in the bile (A_b^{∞}) or urine (A_e^{∞}) of TAM-treated control groups are:

$$A_E^{\infty} = k_E\left(\frac{A}{\alpha} + \frac{B}{\beta}\right) \quad (13)$$

$$A_E^{\infty} = k_E\left(\frac{A}{\alpha} + \frac{B}{\beta} + \frac{C}{\gamma}\right) \quad (14)$$

Warranted by the model selection criteria and time course of DOX in the heart, we chose model III (Fig. 1, excluding the area with the dashed outline) and model IV (Fig. 1, including the area with the dashed outline) to characterize the time course of DOX in myocardial tissue for TAM-treated and control groups, respectively [37]. The purpose of this analysis was to estimate the transfer rate constants of DOX between the central compartment and the myocardial tissue in the TAM-treated group. The intention was to determine the influence of modulation of Pgp by TAM on the magnitude of these rate constants. The rate equations describing the change in the amount of DOX in myocardial tissue of the TAM-treated (Eq. 15) and control (Eq. 16) groups as a function of DOX concentration in the central and peripheral compartments are:

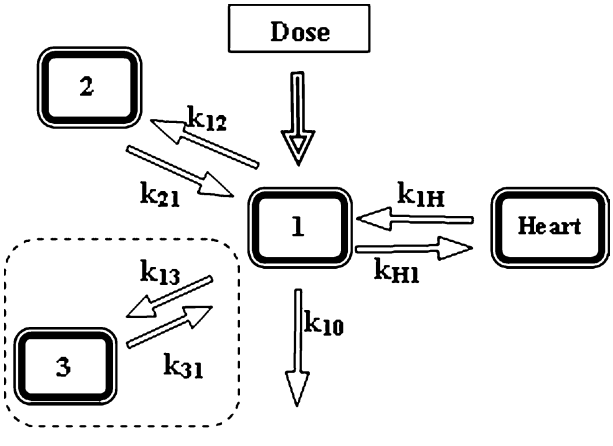

Fig. 1 Diagram of a three-compartment model (model III, area with *dashed outline* excluded), or a four-compartment model (model IV, area with *dashed outline* included) with the heart as the third or fourth compartment, respectively

$$\frac{dA_H}{dt} = k_{1H}A_1 - k_{H1}A_H = k_{1H}\left(Ae^{-\alpha t} + Be^{-\beta t}\right) - k_{H1}A_H \quad (15)$$

$$\frac{dA_H}{dt} = k_{1H}A_1 - k_{H1}A_H = k_{1H}\left(Ae^{-\alpha t} + Be^{-\beta t} + Ce^{-\gamma t}\right) - k_{H1}A_H \quad (16)$$

where, A_H is the amount of DOX in the myocardial tissue at time t, k_{1H} and k_{H1} are first-order transfer rate constants from the central to the myocardial tissue and from the myocardial tissue to the central compartment, respectively.

To establish an equation to define the time course of DOX in myocardial tissue, we integrated Eqs. 15 and 16 with respect to time to develop Eq. 17 for the TAM-treated group and Eq. 18 for the control group.

$$A_H = k_{1H}\left[\left(\frac{Ae^{-\alpha t}}{k_{H1} - \alpha} + \frac{Be^{-\beta t}}{k_{H1} - \beta}\right) - \left(\frac{Ae^{-k_{H1}t}}{k_{H1} - \alpha} + \frac{Be^{-k_{H1}t}}{k_{H1} - \beta}\right)\right] \quad (17)$$

$$A_H = k_{1H}\left[\left(\frac{Ae^{-\alpha t}}{k_{H1} - \alpha} + \frac{Be^{-\beta t}}{k_{H1} - \beta} + \frac{Ce^{-\gamma t}}{k_{H1} - \gamma}\right) - \left(\frac{Ae^{-k_{H1}t}}{k_{H1} - \alpha} + \frac{Be^{-k_{H1}t}}{k_{H1} - \beta} + \frac{Ce^{-k_{H1}t}}{k_{H1} - \gamma}\right)\right]$$

Estimation of all rate constants including k_{1H}, k_{H1}, k_b, and $k_e$was achieved by simultaneous curve fitting of plasma, urine and bile data, or plasma and heart data according to the pertinent integrated equations using WinNonlin.

Results

The body weight as well as food and water consumption of rats treated with corn oil or TAM (1 mg/kg/day) were monitored daily over 10 days. TAM pretreatment caused a statistically significant reduction in daily food (2% body weight) and water (3% body weight) consumption, as well as weight gain (10%) with respect to the control group.

The extended profile of plasma concentration of DOX, up to 24 h, resulted in selection of a three-compartment open model to fit the data from the control group, while a two-compartment model was the appropriate fit to the DOX plasma concentration-time profiles of TAM-treated group. Selection of the models was based solely on the values of AIC and SC, the model selection criteria. For the control group the values of

AIC for two- and three-compartment models were calculated as −25.02 and −44.52 and SC values were −28.22 and −49.33, respectively. The values of AIC for TAM-treated group for two- and three-compartment models were calculated as −28.31 and −27.17 and SC values were −31.5 and −31.9. Thus, we selected the three–compartment model for control and two-compartment model for the TAM-treated group.

The plasma concentration–time profile of both groups is presented in Fig. 2. The estimated pharmacokinetic constants and parameters are compared in Table 1.

TAM pretreatment significantly decreased the elimination rate constant of DOX from the central compartment (k_{10}). The TAM treatment had no significant influence on the distribution rate constant of DOX from the central to the peripheral compartment (k_{12}). However, it reduced significantly the distribution rate constant from the peripheral to the central compartment (k_{21}).

Biliary and urinary data were analyzed according to Eqs 9, 10, 11, 12, 13, 14. The simultaneous curve fitting with plasma data and related equations provided the calculated parameters and constants that are reported in Table 2. The simultaneously fitted composite curves of plasma, bile, and urine data from control and TAM-treated groups are depicted in Fig. 3A.

Approximately 10% of the administered dose of DOX was excreted unchanged in the bile of the control group 6 h after the injection. This amount accounted for approximately 70% of the predicted total unchanged DOX that would be excreted in the bile, A_e^{∞} . TAM pretreatment had no significant effect on the cumulative amount of DOX excreted in the bile in 6 h, and it accounted for 63% of A_e^{∞} (Fig. 4A). The TAM pretreatment reduced, however, the first-order biliary excretion rate constant (k_b) significantly.

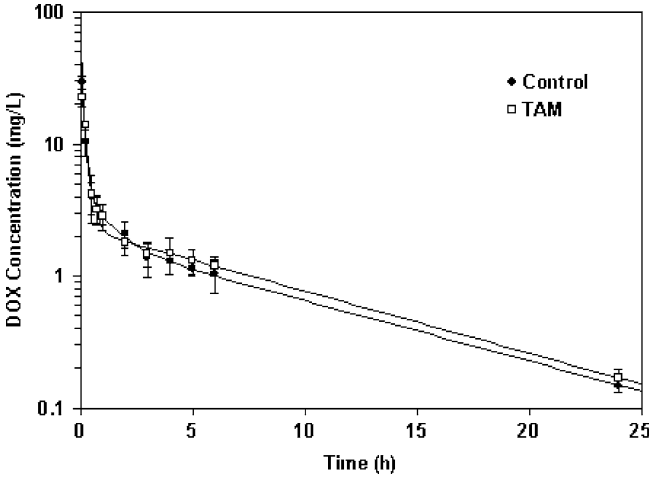

Fig. 2 The plasma concentration-time profile of DOX in the control and TAM-treated groups. Symbols represent the observed data, mean ± SD, $n = 6$ and curves are predicted by the models

Table 1 Summary of the pharmacokinetic parameters and constants of plasma concentrations of DOX in the control and TAM-treated groups

Parameters	Control	TAM-treated
A (mg l^{-1})	51.42 ± 2.95	32.59* ± 4.94
B (mg l^{-1})	3.63 ± 0.32	2.23* ± 0.51
C (mg l^{-1})	1.68 ± 0.46	NA
α (h^{-1})	8.98 ± 0.85	5.21* ± 1.10
β (h^{-1})	0.88 ± 0.45	0.11* ± 0.01
γ (h^{-1})	0.10 ± 0.01	NA
$Cp°$ (mg l^{-1}) (initial plasma concentration)	56.73 ± 5.49	34.81* ± 5.15
V_1 (l) (volume of distribution of central compartment)	0.06 ± 0.01	0.09* ± 0.01
k_{12} (h^{-1})	3.49 ± 0.92	3.59 ± 0.90
k_{21} (h^{-1})	1.48 ± 0.76	0.43* ± 0.06
k_{13} (h^{-1})	2.57 ± 1.15	NA
k_{31} (h^{-1})	0.25 ± 0.06	NA
k_{10} (h^{-1})	2.17 ± 0.25	1.30* ± 0.19
$(T_{1/2})_{k10}$(h) (elimination half-life)	0.32 ± 0.04	0.54* ± 0.08
$(T_{1/2})_{\beta}$ (h) (biological half-life)	0.08 ± 0.01	0.14* ± 0.03
MRT (h) (mean residence time)**	5.93 ± 0.49	6.16 ± 0.50
AUC (mg l^{-1}) (area under the plasma concentration—t curve)	26.27 ± 2.90	27.05 ± 3.86
Cl_T (l/h) (total body clearance)[a]	0.38 ± 0.02	0.37 ± 0.02

Values represent mean ± SD ($n = 6$)
* Significantly different at $P < 0.05$
[a] $\text{MRT} = \frac{\text{AUMC}}{\text{AUC}}$, where AUMC is the area under the moment curve, and $\text{Cl}_T = \frac{\text{Dose}}{\text{AUC}}$

The cumulative amount of DOX excreted unchanged in the urine of the control group was approximately 2.7% of the dose after 24 h from the DOX injection, which constituted close to 90% of the total predicted

Table 2 Comparison of pharmacokinetic parameters of biliary and urinary excretion of DOX in the control and TAM-treated groups obtained from simultaneous curve fitting of plasma, bile and urine data

Parameters	Control	TAM
Bile		
A_b (0–6) Obs. (%dose)	10.70 ± 1.48	10.04 ± 1.53
A_b (0–6) Pred. (%dose)	9.85	10.69
A_b^{∞}(%dose)	14.13	16.83
$A_b(0\text{--}6)/A_b^{\infty}$	0.75	0.60
k_b (1/h)	0.299 ± 0.019	0.211* ± 0.012
Urine		
A_e (0–24) Obs. (%dose)	2.69 ± 0.33	5.26* ± 1.05
A_e (0–24) Pred. (%dose)	2.69	5.74
A_e^{∞}(%dose)	2.99	5.94
$A_e(0\text{--}24)/A_e^{\infty}$	0.90	0.88
k_e (1/h)	0.063 ± 0.007	0.074 ± 0.006
k_m (1/h)	1.901	0.869
k_{10} (1/h)	2.262	1.154
r^2 (Plasma)	0.9996	0.9948
r^2 (Bile)	0.9929	0.9875
r^2 (Urine)	0.9949	0.9856

The observed values represent mean ± SD
Values for k_b and k_e represent mean ± SE
*Significantly different at $P < 0.05$

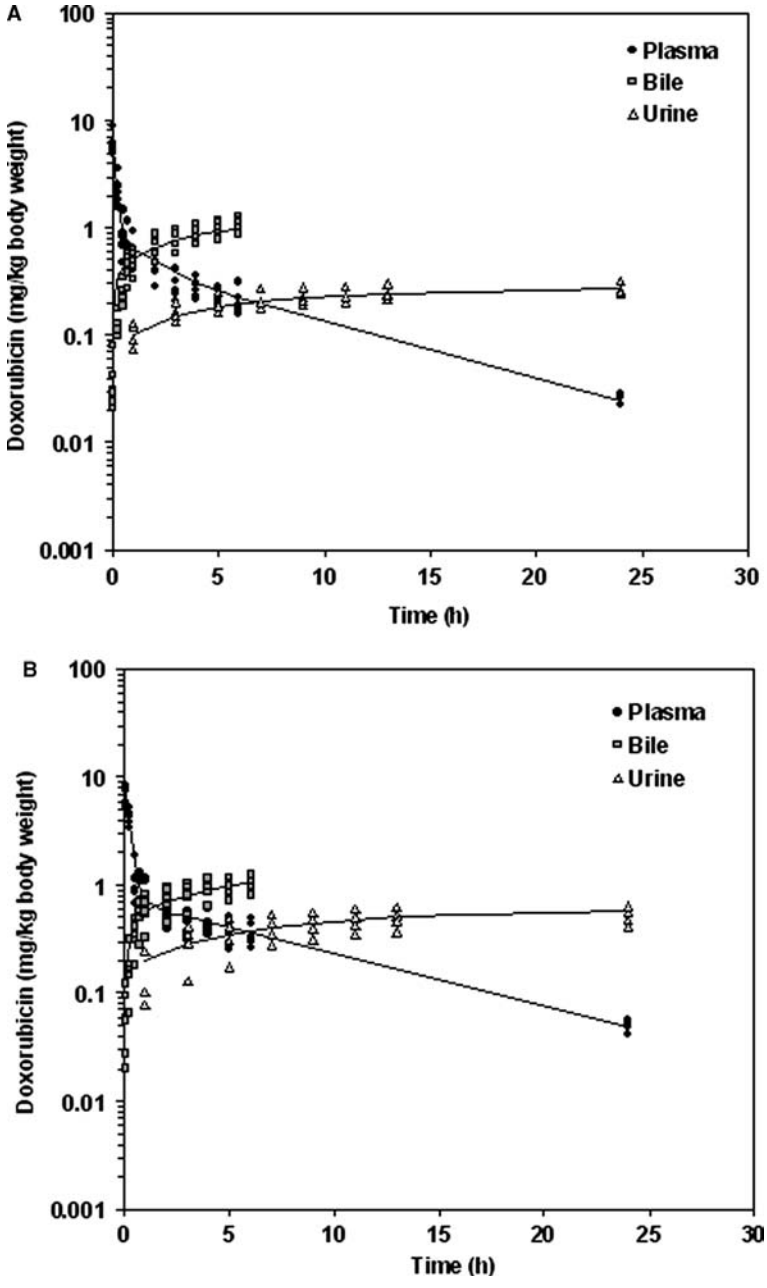

Fig. 3 Simultaneous composite curve fitting of the cumulative amount of DOX in bile and urine with plasma data in the **A** control group and **B** TAM-treated group

amount of unchanged DOX to be ultimately excreted in urine, A_e^{∞}. The fraction of the dose excreted unchanged in the urine of TAM-treated group in 24 h was about 5.26%, which was significantly different from the control group (Fig. 4b). The first-order urinary excretion rate constant (k_e) of DOX in the TAM-treated group was not significantly different from that of the control group.

The time course of DOX distribution in the myocardial tissue of the control and TAM-treated animals are depicted in Fig. 5A. The pharmacokinetic parameters and constants of the myocardial data, according to Eqs. 15, 16, 17, 18, are shown in Table 3. The first-order rate constants between the central and the myocardial compartments (k_{1H} and k_{H1}) were decreased in the TAM-treated group. The treatment also significantly reduced the k_{1H}/k_{H1} ratio with respect to that of the control group. The reduction of C_{max} of the myocardial time course in TAM-treated group was not statistically significant. However, the estimated T_{max} was significantly prolonged in this group.

The area under myocardial tissue concentration of DOX versus time within the first 24 h after the injection was increased 1.22-fold in the TAM-treated group, a statistically significant change. Comparison of the plasma concentration-normalized myocardial data versus time for control and TAM-treated groups is shown in Fig. 5B. The normalized myocardial data with respect to the corresponding plasma concentration, designated as $AUC_{0\text{-}24}$(H/P), revealed a 1.47 increase in the TAM-treated group.

The time course of DOX in the liver and kidney of the control and TAM-treated groups was also evaluated.

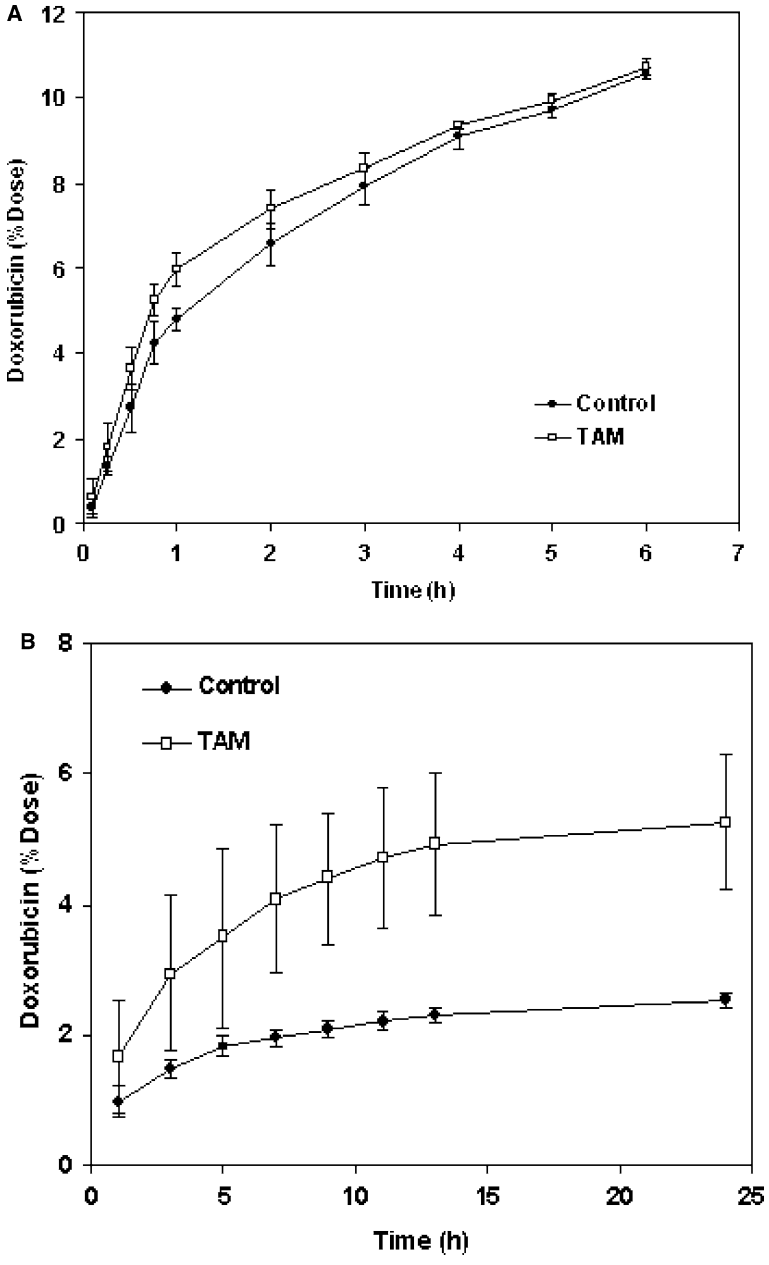

Fig. 4 Comparison of the cumulative amount of DOX excreted in **A** bile and **B** urine of the control and TAM groups

The related AUC and AUC of normalized data with respect to plasma concentration are presented in Table 4. The maximum plasma concentration of DOX in the liver of both groups reached its maximum level 6 h after the injection. The maximum levels of DOX in the kidney of control and TAM-treated groups were reached 1 h and 6 h after the injection, respectively. The level of DOX in the renal tissue of TAM-treated group, as indicated by $AUC_{0\text{-}24}$ values, was significantly increased, by 1.55-fold.

The time course of Pgp-ATPase activity (Fig. 6A) and amount of Pgp in the heart of control 2 and TAM-treated groups were measured 1, 3, 6, 12, and 24 h following the injection of DOX. The data were normalized with respect to the values of control 1 (animals pre-treated with corn oil and receiving normal saline instead of DOX). The Pgp-ATPase activity in control 2 was reduced by about 96% 1 h after DOX administration. The reduction was followed by a steady increase in the activity that reached 74% and 100% of the basal level 12 h and 24 h following the injection of DOX. The initial reduction of Pgp activity in TAM-treated group was at 60% of the basal level. The activity declined to 20% of the basal activity after 6 h and showed no significant change during the rest of the course of the study (Fig. 6A). The area under the curves of Pgp-ATPase activity time ($AUC_{Activity\ 0\text{-}24}$) following DOX administration to control 2 and TAM-treated groups are compared in Table 5. The calculated AUC values of the TAM-treated group were significantly lower than in

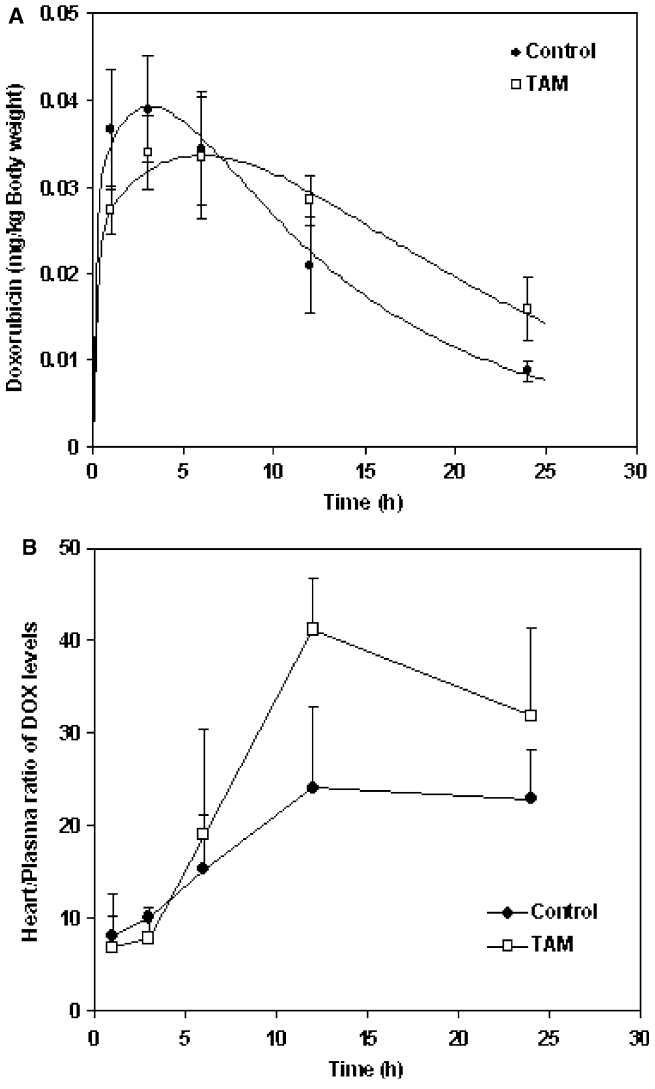

Fig. 5 Comparison of the time course of **A** myocardial levels of DOX and **B** heart-to-plasma ratio of DOX in the control and TAM-treated groups; symbols represent mean ($n=4$) and SD of observed values, and curves are predicted by the models

control 2, indicating an overall inhibitory effect of TAM on Pgp-ATPase activity under the protocol of this study. The pretreatment had no significant effect on the amount of Pgp in the heart within the first 24 h after the DOX injection (data not shown).

We chose the sarcoplasmic reticulum (SR) Ca^{2+} - ATPase (SERCA) activity of myocardial tissue as the biomarker of DOX cardiotoxicity. The time course of SERCA of control 2 is compared to that of the TAM-treated group in Fig. 6B. The initial decline in the activity of the TAM-treated group was about 40%. The SERCA activity in the control group showed a biphasic pattern within the 24-h period following DOX administration. In the TAM-treated group, the activity declined steadily over the 24-h period with a slope value of −1.25. The areas under the curves of the SERCA activity-time curve following DOX administration to control 2 and the TAM-treated groups are compared in Table 5. The TAM-treated group demonstrated a 15% reduction in $AUC_{Activity\ \ 0\text{-}24}$ in comparison with that of control 2, an indication of increased toxicity.

Table 3 Comparison of pharmacokinetic parameters obtained from myocardial distribution of DOX in control and TAM groups obtained from simultaneous curve-fitting of plasma and heart data

Parameters	Control	TAM
k_{1H}(1/h)	0.0172 ± 0.0018	0.0123* ± 0.0025
k_{H1} (1/h)	0.1526 ± 0.0152	0.0978* ± 0.0240
k_{H1}/ k_{1H}	8.86 ± 0.10	7.88 * ± 0.50
$AUC_{0\text{-}24}$ (ng.h/mg)	347.04 ± 21.52	424.68* ± 28.50
$AUC_{0\text{-}24}$(H/P) (h)	921.84 ± 213.48	1353.79* ± 191.70
C_{max} (mg/kg)	0.039 ± 0.007	0.036 ± .006
T_{max} (h)	3.28 ± 0.41	5.81* ± 0.32
k_{10} (1/h)	1.958 ± 0.205	1.350 ± 0.141
r^2 (Plasma)	0.9949	0.9854
r^2 (Heart)	0.9812	0.9852

Values represent mean ± SD
*Significantly different at $P<0.05$

Discussion

The present study was initiated based on the premise that an inhibitor of Pgp not only reverses Pgp-dependent multidrug resistance and improves the potency of chemotherapeutic agents, but also influences normal cellular uptake and may cause organ toxicity. This possible drug-to-drug interaction is more common for cancer chemotherapeutic agents, such as doxorubicin, which are Pgp substrate.

Compartmental analysis of the data suggested a reduction in the overall elimination rate constant (k_{10}) and the distribution rate constant from the peripheral compartment to the central compartment (k_{21}). Such an effect could partially be attributed to the inhibitory effect of the Pgp modulators in the body. Our results are consistent with clinical reports on the effect of TAM on pharmacokinetics of DOX [38]. The lack of significant change in the plasma pharmacokinetics of DOX has also been reported for therapeutic doses of other Pgp modulators [39, 40]. Our observation in conjunction with reported data by other investigators confirmed that the

Table 4 Comparison of the extent of availability of DOX in the liver and kidneys of the control and TAM-treated groups

Parameters	Control	TAM
Liver		
$AUC_{0\text{-}24}$ (ng.h/mg)	181.22 ± 36.68	132.67 ± 14.30
$AUC_{0\text{-}24}$(L/P) (h)	620.49 ± 225.68	457.38 ± 124.32
Kidney		
$AUC_{0\text{-}24}$ (ng.h/mg)	78.88 ± 1.90	121.38* ± 2.09
$AUC_{0\text{-}24}$(K/P) (h)	222.61 ± 49.03	355.32* ± 81.82

Values represent mean ± SD ($n=4$)
* Significantly different at $P<0.05$

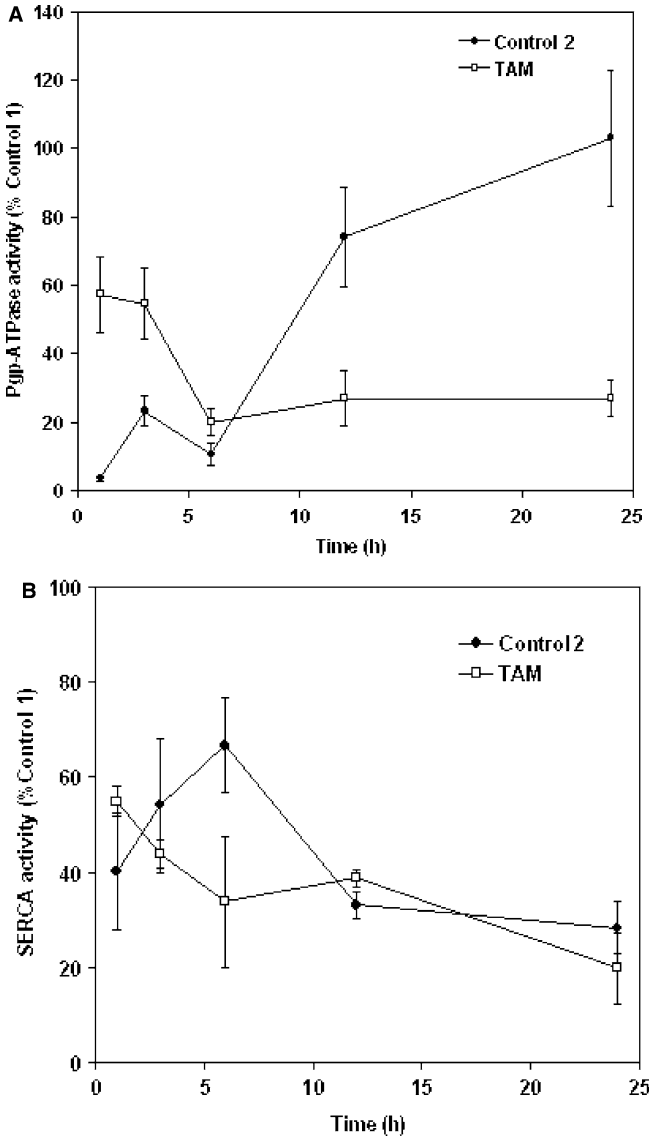

Fig. 6 Comparison of the time course of **A** Pgp-ATPase activity, and **B** SERCA activity in the heart of control 2 and TAM-pretreated group following DOX administration

modulatory effects of Pgp modulators should be evaluated in the target organ rather than in the plasma.

Biliary and urinary excretion of DOX in the control and the TAM-treated groups was investigated by simultaneous curve fitting of the data from bile, urine, and plasma. The results obtained from the control group were consistent with those reported in the literature [41–43]. The first-order biliary elimination rate constant (k_b) was significantly decreased by 29% in the TAM-treated group. The reduction was estimated in comparison to that of the control group. This reduction could be attributed to the inhibitory effect of TAM on Pgp located on biliary canicular membranes. However, the lack of significant difference between the cumulative amount of DOX excreted in the bile of the control and TAM-treated groups suggests that additional effects of TAM are involved in the modification of pharmacokinetics of DOX in the liver, and this modification might be related to the reduction of tissue binding of DOX in the liver or a reduction in the extent of DOX metabolism. The estimated first-order metabolic rate constant of DOX in TAM-treated group was also reduced.

In contrast to the bile data, comparison of the results from urinary excretion of DOX revealed a marked increase in the cumulative DOX excretion in the urine of the TAM-treated group. However, TAM pretreatment did not alter the first-order urinary excretion rate constant (k_e) significantly. The increase in excretion of DOX might be attributed to the vasodilation properties of TAM [44, 45]. TAM vasodilation activity has been identified as an endothelium- and nitric-oxide-dependent mechanism, with a direct effect on the smooth muscle and independent of calcium [45].

In view of the differences in the results of DOX accumulation in the hepatic and renal tissues, it was concluded that the effect of TAM pretreatment on DOX accumulation in the liver and kidneys is organ-dependent. The results obtained from the heart data also confirmed that the TAM influence on DOX accumulation is organ-dependent .

The compartmental analysis of the data revealed that TAM pretreatment significantly decreases k_{1H} and k_{H1}, as well as the k_{H1}/k_{1H} ratio. This is in agreement with the notion that TAM, owing to its lipophilic nature, can interact extensively with the lipid membranes and change their fluidity. It is also consistent with the prolonged T_{max} estimated for DOX in the TAM group with respect to that of the control group. To determine whether factors other than membrane rigidity influence the extent of accumulation of DOX in the heart, the ratio of k_{H1}/k_{1H} was estimated and considered to be the effect of transporters. The reduction in the k_{H1}/k_{1H} ratio in the TAM group is due to reduction of k_{H1} that is associated with its net inhibitory effect on Pgp efflux activity.

The time course of the myocardial SR Ca^{2+} -ATPase (SERCA) activity, the toxicodynamic biomarker of the present study, showed a sharp reduction in the enzyme activity the first hour following DOX administration. The time course of the myocardial SERCA activity in the control group showed a biphasic pattern over the course of this study, which was consistent with the results of a published in vitro study that suggested a

Table 5 Comparison of the area under the curves of myocardial Pgp-ATPase activity following DOX administration to control 2, TAM

Treatment	Group	$AUC_{Activity\ 0\text{-}24}$ (%Activity.h)	
		Pgp-ATPase	SERCA
DOX/Corn oil	Control 2	1445.90 ± 275.22	1033.03 ± 75.25
DOX/TAM	TAM	766.37* ± 162.13	883.25* ± 34.79

Values represent mean ± SD ($n = 4$)
*Significantly different at $P < 0.05$

similar biphasic pattern characterized by an early and a delayed positive inotropic effect of DOX [46]. The authors attributed the early phase to the release of Ca^{2+} from the sarcoplasmic reticulum, and the late phase to Ca^{2+} influx through slow Ca^{2+} channels. TAM pretreatment modified the biphasic profile of the time course of myocardial SERCA activity of the control group into a gradual decline of enzyme activity against time. Although the cause of this TAM effect is not clear at this time, it might be due to its interaction with lipid bilayers of sarcoplasmic reticulum. The $AUC_{0\text{-}24}$ of SERCA activity was reduced by 15% with respect to that of control 2, which indicates an increase in the extent of DOX-induced cardiotoxicity (Table 5). Considering our results from the effect of TAM on DOX accumulation in the myocardial tissue, the increase in cardiotoxicity can only be related to the net inhibitory effect of TAM on the efflux activity of Pgp.

The $AUC_{0\text{-}24}$ of the time course of myocardial Pgp-ATPase activity was reduced by 47% in the TAM-treated group, suggesting an inhibitory effect for TAM. The amount of myocardial Pgp detected within the 24-h period following DOX administration was comparable in both groups and showed no significant deviation from the basal levels of the protein. These results suggested that the pretreatments had no inducing or suppressing effect on myocardial Pgp expression according to the protocol of present study.

The existence of a delay in toxicodynamic response with respect to the drug concentration can be established by the characteristics of hysteresis. This delay can be indicated by a counter-clockwise hysteresis [47] obtained from the plot of response-versus-drug concentration. The delayed response may be due to a slowly formed active/toxic metabolite, or the drug acting on receptors in a deep compartment, or both. Figure 7 illustrates the area under the curve of SERCA inhibition versus the amount of DOX in the heart of the control 2 and TAM-treated groups. The arrows point out the direction of the curves, which is counterclockwise for both groups.

The correlation of SERCA activity as the toxicodynamic parameter of this investigation with the calculated pharmacokinetic parameters was also investigated. Among all pharmacokinetic parameters, the AUC of the heart-to-plasma ratio of DOX levels exhibited meaningful correlation with AUC of SERCA activity (Fig. 8A). The slope of the lines indicates the extent of cardiotoxicity with respect to the heart-to-plasma ratio. The slopes of the linear segments of the curves were calculated as 0.516 and 0.300 for the control and TAM-treated groups, respectively. The smaller slope would correspond to higher toxicity.

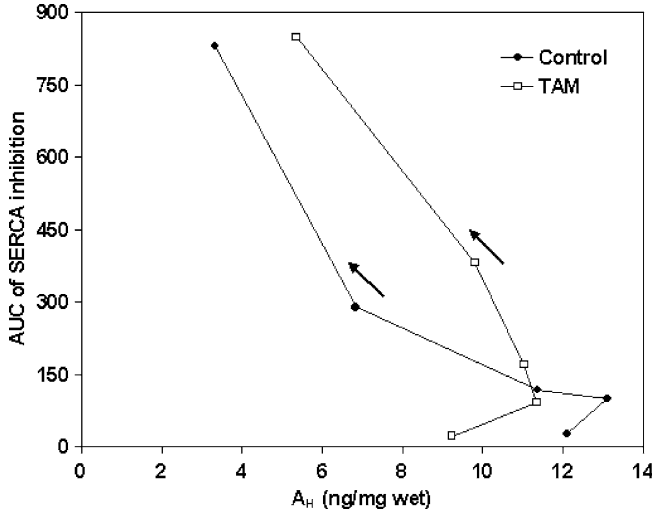

Fig. 7 Counter-clockwise hysteresis of AUC of SERCA inhibition versus amount of DOX in the heart of the control 2 and TAM groups

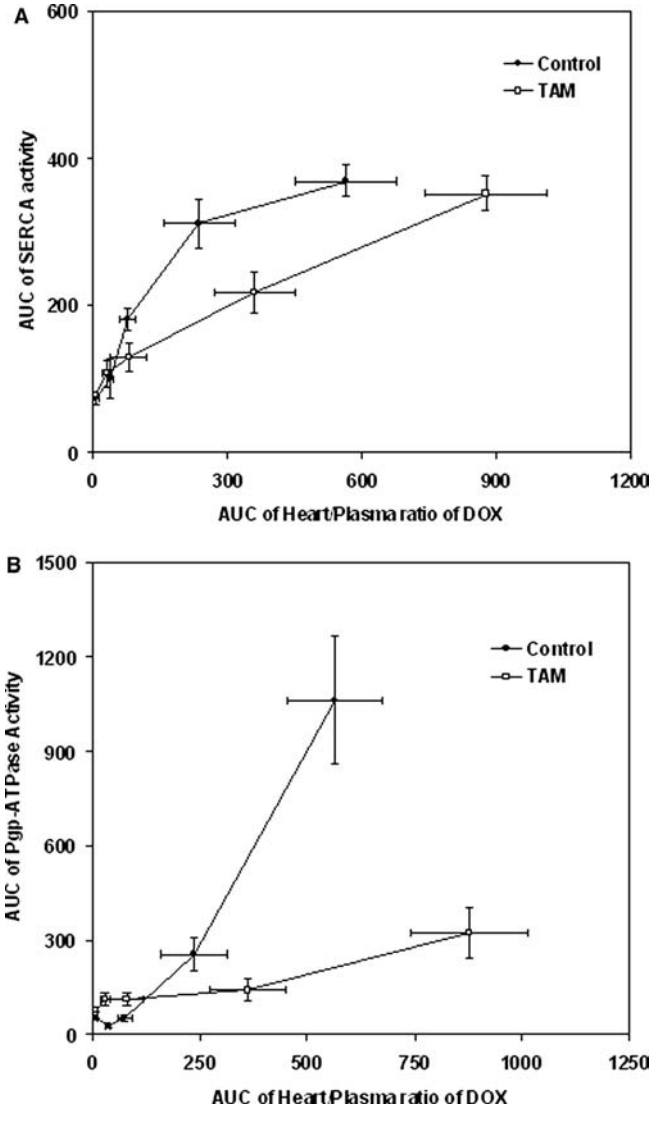

Fig. 8 Correlation of the AUC of myocardial **A** SERCA activity and **B** Pgp-ATPase activity with the AUC of heart-to-plasma ratio of DOX in the control and TAM groups. The correlation coefficients for the control and TAM-treated groups in **A** are 0.916 and 0.992 and in **B** 0.980 and 0.973, respectively

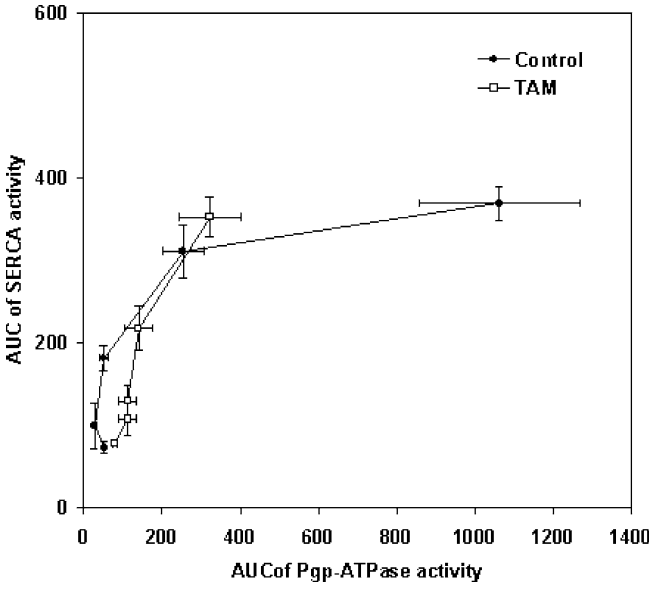

Fig. 9 Correlation of the AUC of myocardial SERCA activity with the AUC of myocardial Pgp-ATPase activity in the control and TAM groups following DOX administration. The correlation coefficients for the control and TAM groups are 0.820, and 0.959, respectively

The modulatory effect of TAM on myocardial Pgp-ATPase activity with respect to the levels of DOX accumulation in the heart is presented in Fig. 8B. The extent of modulation can be determined by comparing the slopes of the curves from TAM-treated groups with those of the control group. Slopes with lower values than those of the control group indicate a net inhibitory effect, and slope values exceeding the control values suggest a net stimulatory impact. Slopes associated with the lines in Fig. 8B were calculated as 1.881 and 0.258 for the control and TAM groups, respectively.

To explore the relationship between the myocardial SR Ca^{2+} -ATPase activity with that of Pgp-ATPase, the corresponding AUCs were plotted against each other as presented in Fig. 9. The plot provides the functional interrelationship between the two proteins in DOX-induced cardiotoxicity. The interrelationship between the AUCs of SERCA and Pgp-ATPase activities implies that the Pgp-ATPase activity has a direct relationship with the extent of SERCA activity.

In conclusion, our results established a correlation between the modulatory effect of TAM on Pgp activity in the heart (as determined by myocardial Pgp ATPase activity) and DOX cardiotoxicity (as determined by myocardial SERCA activity) in vivo. The proposed mechanism might be an underlying factor in the interaction between Pgp modulators and DOX accumulation in myocardial tissue and the consequent extent of cardiotoxicity. We also showed that the extent of tissue accumulation of DOX cannot be represented by the AUC of the plasma. Although the design of this study reflects acute cotreatment of DOX and TAM, cotherapy of DOX with Pgp modulators such as TAM should be recommended with caution. Depending upon the concentration of the modulator in the heart and its influence as an inhibitor of Pgp, and the timing of DOX administration in a multiple dosing regimen of a modulator, an unexpected cardiotoxic response may occur, which would be due to the accumulation of DOX in the heart.

Acknowledgements This project was supported by the SAHAG Foundation and completed at Northeastern University, Boston, Massachusetts.

References

1. Chang G (2003) Multidrug resistance ABC transporters. FEBS Let 555: 102–105
2. Smit JW, Duin E, Steen H, Oosting R, Roggeveld J, Meijer DKF (1998) Interactions between P-glycoprotein substrates and other cationic drugs at the hepatic excretory level. Br J Pharmacol 123: 361–370
3. Cordon-Cardo C, O'brien JP, Boccia J, Casals D, Bertino R, Melamed MR (1990) Expression of the multidrug resistance gene product (P-glycoprotein) in human normal and tumor tissues. J Histochem Cytochem 38: 1277–1287
4. Thiebaut F, Tsuruo T, Hamada H, Gottesman MM, Pastan I, Willingham MC (1987) Cellular localization of the multidrug-resistance gene product P-glycoprotein in normal human tissues. Proc Natl Acad Sci USA 84: 7735–7738
5. Stephens RH, O'neill CA, Warhurst A, Carlson GL, Rowland M, Warhurst G (2000) Kinetic profiling of P-glycoprotein-mediated drug efflux in rat and human intestinal epithelia. J Pharmacol Exp Ther 296: 584–591
6. Thiebaut F, Tsuruo T, Hamada H, Gottesman M, Pastan I, Willingham C (1989) Immunohistochemical localization in normal tissues of different epitopes in the multidrug transport protein P170: evidence for localization in brain capillaries and crossreactivity of one antibody with a muscle protein. J Histochem Cytochem 37: 159–164
7. Ernest S, Bello-Reuss E (1998) P-glycoprotein functions and substrates: possible roles of MDR1 gene in the kidney. Kidney Int 53(65):S11-S17
8. Hori R, Okamura N, Aina T, Tanigawara Y (1993) Role of P-glycoprotein in renal tubular secretion of digoxin in the isolated perfused rat kidney. J Pharmacol Exp Ther 266: 1620–1625
9. Karyekar CS, Eddington ND, Garimella TS, Gubbins PO, Dowling TC (2003) Evaluation of P-glycoprotein-mediated renal drug interactions in an MDR1-MDCK model. Pharmacotherapy 23:436–42
10. Garrigues A, Loiseau N, Delaforge M, Ferte J, Garrigos M, Andre F, Orlowski S (2002) Characterization of two pharmacophores on the multidrug transporter P-glycoprotein. 62:1288–1298
11. Smit JW, Duin E, Steen H, Oosting R, Roggeveld J, Meijer DKF (1998) Interactions between P-glycoprotein substrates and other cationic drugs at the hepatic excretory level. Br J Pharmacol 123: 361–370
12. Darvari R, Boroujerdi M (2004) Concentration dependency of modulatory effect of amlodipine on P-glycoprotein efflux activity of doxorubicin—a comparison with tamoxifen. J Pharm Pharmacol 56:985–991
13. Estevez MD, Wolf A, Schramm U (2000) Effect of PSC 833, verapamil and amiodarone on adriamycin toxicity in cultured rat cardiomyocytes. Toxicol in Vitro 14: 17–23
14. Kiss Z, Crilly KS (1995) Tamoxifen inhibits uptake and metabolism of ethanolamine and choline in multidrug-resistant, but not in drug-sensitive, MCF-7 human breast carcinoma cells. FEBS Let 360: 165–168
15. Relling MV (1996) Are the major effects of P-glycoprotein modulators due to altered pharmacokinetics of anticancer drugs? Ther Drug Monit 18: 350–356

16. Wielinga PR, Westerhoff HV, Lankelma J (2000) The relative importance of passive and P-glycoprotein mediated anthracycline efflux from multidrug-resistant cells. Eur J Biochem 267: 649–657
17. Priebe W, Perez-Soler R (1993) Design and tumor targeting of anthracyclines able to overcome multidrug resistance: a double advantage approach. Pharmacol Therapeut 60: 215–234
18. Maruyama Y, Murohashi I, Nara N, Aoki N (1989) Effect of verapamil on the cellular accumulation of daunorubicin in blast cells and on the chemosensitivity of leukemic blast progenitors in acute myelogenous leukemia. Br J Haematol 72: 357–362
19. Frezard, F, Pereira-Maia E, Quidu P, Priebe W, Garnier-Suillerot A (2001) P-glycoprotein preferentially effluxes anthracyclines containing free basic versus charged amine. Eur J Biochem 268: 1561–1567
20. Bellamy WT, Peng YM, Odeleye A, Ellsworth L, Xu MJ, Grogan TM, Weinstein, RS (1995) Cardiotoxicity in the SCID mouse following administration of doxorubicin and cyclosporin A. Anticancer Drugs 6: 736–743
21. Estevez MD, Wolf A, Schramm U (2000) Effect of PSC 833, verapamil and amiodarone on adriamycin toxicity in cultured rat cardiomyocytes. Toxicol in Vitro 14: 17–23
22. Sridhar R, Dwivedi C, Anderson J, Baker PB, Sharma HM, Desai P, Engineer FN (1992) Effects of verapamil on the acute toxicity of doxorubicin in vivo. Reports 84: 1653–1660
23. Vaidyanathan S, Boroujerdi M (2000) Effect of tamoxifen pretreatment on the pharmacokinetics, metabolism and cardiotoxicity of doxorubicin in female rats. Cancer Chemother Pharmacol 46: 185–192
24. Kayyali R, Marriott C, Wiseman H (1994) Tamoxifen decreases drug efflux from liposomes: relevance to its ability to reverse multidrug resistance in cancer cells. FEBS Let 344: 221–224
25. Lavie Y, Cao HT, Volner A, Lucci A, Han TY, Geffen V, Giuliano AE, Cabot, MC (1997) Agents that reverse multidrug resistance, tamoxifen, verapamil, and cyclosporin A, block glycosphingolipid metabolism by inhibiting ceramide glycosylation in human cancer cells. J Biol Chem 272: 1682–1687
26. Rao US, Fine RL, Scarborough GA (1994) Antiestrogens and steroid hormones: substrates of the human p-glycoprotein. Biomed Pharmacol 48: 287–292
27. Kiss Z, Tomono M, Anderson (1994) WB Phorbol ester selectively stimulates the phospholipase D-mediated hydrolysis of phosphatidylethanolamine in multidrug-resistant MCF-7 human breast carcinoma cells. Biochem J 302: 649–654
28. Kiss Z, Crilly, KS (1995) Tamoxifen inhibits uptake and metabolism of ethanolamine and choline in multidrug-resistant, but not in drug-sensitive, MCF-7 human breast carcinoma cells. FEBS Lett 360: 165–168
29. Gustafson DL, Swanson JD, Pristos CA (1993) Modulation of glutathione and glutathione dependent antioxidant enzymes in the mouse heart following doxorubicin therapy. Free Radic Res 19: 111–120
30. Andersen A, Warren DJ, Slordal LA (1993) Sensitive and simple high-performance liquid chromatographic method for the determination of doxorubicin and its metabolites in plasma. Ther Drug Monit 15: 455–461
31. Simonides WS, van Hardeveled C (1990) An assay for sarcoplasmaic reticulum Ca2+-ATPase activity in muscle homogenates. Anal Biochem 191: 321–331
32. Saheki S, Takeda A, Shimazu T (1985) Assay of inorganic phosphate in the mild pH range, suitable for measurement of glycogen phosphorylase activity. Anal Chem 148: 277–281
33. Kokubu N, Cohen D, Watanabe T (1997) Functional modulation of ATPase of P-glycoprotein by C219, a monoclonal antibody against P-glycoprotein. Biochem Biophys Res Commun 230: 398–401
34. Friedlander ML, Bell DR, Leary J, Davey RA (1989) Comparison of Western blot analysis and immunocytochemical detection of P-glycoprotein in multidrug resistant cells. J Clin Pathol 42: 719–722
35. Ludden TM, Beal SL, Sheiner LB (1994) Comparison of the Akaike Information Criterion, the Schwarz criterion and the F test as guides to model selection. J Pharmacokin Biopharm 22: 431–445
36. Boroujerdi M (2001) (eds) Pharmacokinetics: principles and applications. McGraw-Hill New York
37. Kates RE, Jaillon PA (1980) Model to describe myocardial drug disposition in the dog. J Pharmacol Exp Ther 214: 31–36
38. El Yazigi A, Berry J, Ezzat A, Wahab FA (1997) Effect of tamoxifen on the pharmacokinetics of doxorubicin in patients with non-Hodgkin's lymphoma. Ther Drug Monit 19: 632–636
39. Relling MV (1996) Are the major effects of P-glycoprotein modulators due to altered pharmacokinetics of anticancer drugs? Ther Drug Monit 18: 350–356
40. Sparreboom A, Planting AS, Jewell RC, van der Burg ME, van der Gaast A, de Bruijn P, Loos WJ, Nooter K, Chandler LH, Paul EM, Wissel PS, Verweij (1999) Clinical pharmacokinetics of doxorubicin in combination with GF120918, a potent inhibitor of MDR1 P-glycoprotein. Anticancer Drugs 10: 719–728
41. Behnia K, Boroujerdi M (1998) Investigation of the enterohepatic recirculation of Adriamycin and its metabolites by a linked-rat model. Cancer Chemother Pharmacol 41: 370–376
42. Maniez-Devos DM, Baurain R, Lesxe M, Trouet A (1986) Doxorubicin and daunorubicin plasmatic, hepatic and renal disposition in the rabbit with or without enterohepatic circulation. J Pharmacol 17: 1–13
43. Riggs CE Jr, Benjamin RS, Serpick AA, Bachur NR (1977) Billiary disposition of adriamycin. Clin Pharmacol Ther 22: 234–241
44. Park S, Kim B, Kim J, Won KJ, Lee S, Kwon S, Cho S (2003) Tamoxifen induces vasorelaxation via inhibition of mitogen-activated protein kinase in rat aortic smooth muscle. J Vet Med Sci 65:1155–1160
45. Figtree GA, Webb CM, Collins P (2000) Tamoxifen acutely relaxes coronary arteries by an endothelium-, nitric oxide-, and estrogen receptor-dependent mechanism. J Pharmacol Exp Ther 295: 519–523
46. Temma K, Chungun A, Hara Y, Sasaki T, Kondo H (1999) Biphasic positive inotropic actions of doxorubicin in isolated guinea pig hearts. Relation to Ca^{2+} release from the sarcoplasmic reticulum. Gen Pharmacol 33: 229–236
47. Chu KM, Hu OY, Shieh SM (1999) Cardiovascular effect and simultaneous pharmacokinetic and pharmacodynamic modeling of pimobendan in healthy normal subjects. Drug Metab Dispos 27: 701–709